Chapter 1
Digital Rolling Test of Cycloidal Hypoid Gears Based on Measuring Tooth Surface Data

Yongxiang Liu, Jinfu Du, and Kai Liu

Abstract A digital gear rolling test method based on the real tooth surface measuring data is proposed in this study to obtain the actual tooth surface meshing situation. First, the non-uniform rational b-spline (NURBS) technique is used to reconstruct the real tooth surface. Secondly, the instant meshing point is accurately calculated, and the instant contact ellipse corresponding to each meshing point is solved, then the contact pattern composed of the contact ellipses of the entire tooth surface is obtained. Third, the transmission error is calculated based on the theoretical and actual rotation angles of each meshing point. Finally, a pair of cycloidal hypoid gears is taken as an example to verify the feasibility of the above method.

Keywords Cycloid hypoid gear · Measuring tooth · Real tooth surface · Digital rolling test

1.1 Introduction

Cycloidal hypoid gears have many advantages such as high bearing capacity, stable meshing transmission, and high processing efficiency, which are widely used in modern industry. Its transmission performance depends on the accurate realization of the design tooth surface [1, 2], but the manufacturing error is inevitable, which will cause tooth surface deviation. When The technician corrects it, they rely too much on experience and have certain subjectivity. With the development of modern surface modeling technology and precision measurement technology, high precision digital inversion of the real tooth surface is possible, and digital rolling test technology is realized.

Y. Liu · J. Du (✉) · K. Liu
School of Mechanical and Precision Instrument Engineering, Xi'an University of Technology, Xi'an 710048, China
e-mail: dujinfu@xaut.edu.cn

K. Liu
e-mail: kliu@mail.xaut.edu.cn

© The Author(s), under exclusive license to Springer Nature Singapore Pte Ltd. 2022

J. Tan (ed.), *Advances in Mechanical Design*, Mechanisms and Machine Science 111,
https://doi.org/10.1007/978-981-16-7381-8_1

The digital rolling test of real tooth surface replaces the traditional rolling test, which not only avoids the subjective error but also is easy to realize the automatic correction of tooth surface error, which will be beneficial to closed-loop manufacturing. Many scholars have conducted a lot of fruitful research on digital modeling of tooth surfaces and real tooth contact analysis. Litvin et al. [3] calculate the contact ellipse through the derivation of principal curvature and relative curvature. Sun et al. [4] proposed the zero-gap method and the tangent method based on the real tooth surface to solve the instant meshing point. Su et al. [5] proposed to use the angle between the connection line of the two meshing points and the normal line of a meshing point as the objective function to find the instant meshing point. Liu et al. [6] proposed to solve the instant meshing point by solving the distance of grid points. Zhang et al. [7] used the measurement data of the tooth surface to fit the real tooth surface of the spiral bevel gear by the NURBS method. Du et al. [8] also used NURBS to realize the real tooth surface meshing simulation of cycloidal hypoid gear. Wang et al. [9] used the search method to obtain the contact ellipse boundary. The above research has well the foundation for the digital rolling test of gears, but the solving process of the real tooth surface pattern is too complicated, and the quadratic approximation of the curved surface has certain errors.

Herein, a novel digital rolling test method of real tooth surfaces based on the measurement data is proposed in this study. This method uses a digital search method to accurately calculate the contact pattern and transmission error of the real tooth surfaces, which avoid complicated curvature derivation and can significantly reduce the equipment and time costs in the closed-loop manufacturing of cycloidal hypoid gears.

1.2 Tooth Surface Measuring Points

The distribution of tooth surface measuring points will directly affect the accuracy of modeling. This study refers to the measuring center of Klingelnberg P series and uses 15 × 15 measuring points. As shown in Fig. 1.1, u is the tooth height direction, and v is the tooth width direction.

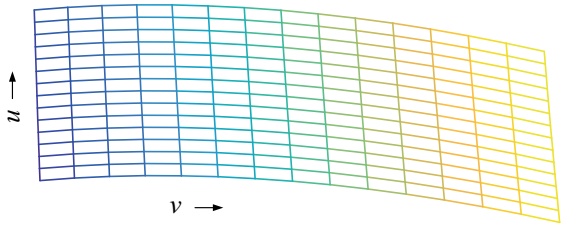

Fig. 1.1 Distribution of measuring points

1.3 Real Tooth Surface Modeling

The mathematical equation of NURBS surface is as follows:

$$P(u, v) = \frac{\sum_{i=0}^{m} \sum_{j=0}^{n} w_{i,j} d_{i,j} N_{i,j}(u) N_{i,j}(v)}{\sum_{i=0}^{m} \sum_{j=0}^{n} w_{i,j} N_{i,k}(u) N_{j,l}(v)} \tag{1.1}$$

where u and v are parameters of the tooth surface, $w_{i,j}$ is the weight factor, $d_{i,j}$ is the control vertex, $N_{i,k}(u)$ and $N_{j,l}(v)$ are the b-spline basis function.

The real tooth surface modeling has the following steps:

Step 1: Take 15 columns of measuring points in the u direction, each column measuring points will get 17 control vertices and weighting factors according to the curve inverse calculation algorithm.
Step 2: Take out 17 rows of control vertices and weighting factors from the 17 × 15 data obtained in the previous step in the v direction, and each row will get 17 control vertices and weighting factors according to the curve inverse calculation algorithm again.
Step 3: The mathematical equation of the real tooth surface is obtained by substituting 17 × 17 control vertices, weight factors, and b-spline basis functions obtained by the search into Eq. (1.1), and the model is established.

Taking cycloidal hypoid gear as an example, (detailed parameters are in Tables 1.1, 1.2, and 1.3), the real tooth surface model is obtained by taking 15 × 15 measuring points on the theoretical tooth surface. As shown in Fig. 1.2.

The reconstructed real tooth surface model passes through 15 × 15 measuring points, but the curved surfaces other than the measuring points are obtained by a fitting algorithm. Therefore, it is necessary to verify the fitting accuracy of these regions, which are the blue regions in Fig. 1.3.

The verification idea is to compare the deviation of the 14 × 14 grid center point on the real tooth surface and the theoretical tooth surface. The verification process has the following steps:

Table 1.1 Basic parameters

Parameters	Pinion	Gear
Shaft/(°)	90	
Offset/mm	40	
Mean normal/mm	6.065	
Number of teeth	12	49
Face width/mm	65	60
Pinch cone angl/(°)	18.2058	71.3535
Mean spiral angle/(°)	42.922LH	30RH
Mean radius/mm	49.692	171.575

Table 1.2 Tool parameters

Parameters	Pinion		Gear	
	Convex	Concave	Convex	Concave
Cutter radius/mm	135	135.397	135	135.461
Profile angle/(°)	21	−19	19	−21
Eccentricity/(°)	0	3.872	0	3.311
Initial setting angle/(°)	0	48	0	−48
Offset/(°)	6.449	6.43	−6.449	−6.427
Orientation angle/(°)	0	160.288	0	−160.901

Table 1.3 Machine settings

Parameters	Pinion	Gear
Swivel angle/(°)	20.51	159.49
Radial setting/mm	172.038	172.038
Initial cradle angle setting/(°)	56.983	−44.061
Vertical offset/mm	35.697	4.115
Increment of machine center to back/mm	15.728	−10.982
Sliding base feed setting/mm	−3.034	8.526
Machine root angle/(°)	18.206	71.354
Roll ratio	4.169	1.021

Step 1: According to the NURBS surface forward calculation algorithm, the three-dimensional coordinates of the center point of the real tooth surface mesh are obtained.
Step 2: Using the theoretical tooth surface equation, the Z coordinates are calculated by substituting X and Y, which are the values of the real tooth surface.
Step 3: Calculating the distance between two points, the error graph is drawn, as shown in Fig. 1.4. The fitting error is the maximum distance in each column in the u direction.

1.4 Digital Rolling Test Method

1.4.1 Coordinate Transformation

The pinion and gear are in a meshing state through coordinate transformation.

The coordinate transformation process is as follows according to Fig. 1.5.

$$M_{s\_p1} = M_{sr}\, M_{rq}\, M_{qp}\, M_{p1}\, P_1(u_1, v_1) \tag{1.2}$$

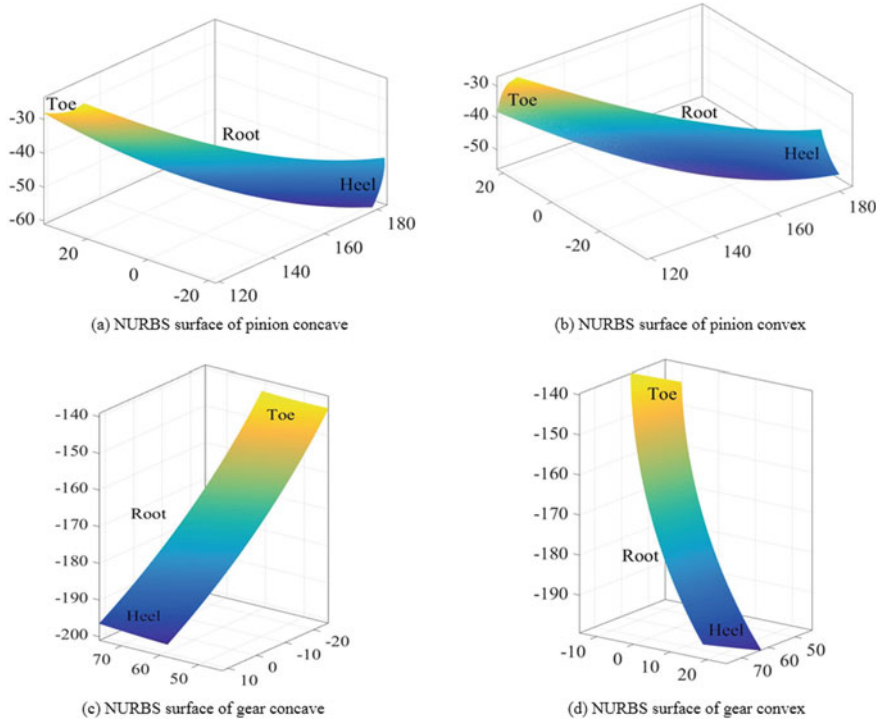

Fig. 1.2 Real tooth surface model

Fig. 1.3 Schematic diagram of the verification area on the real tooth surface model

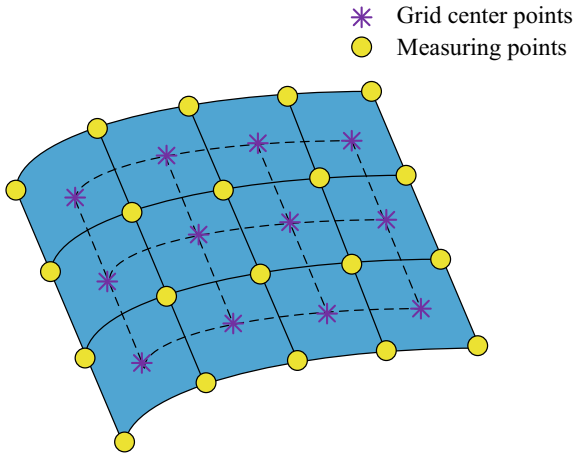

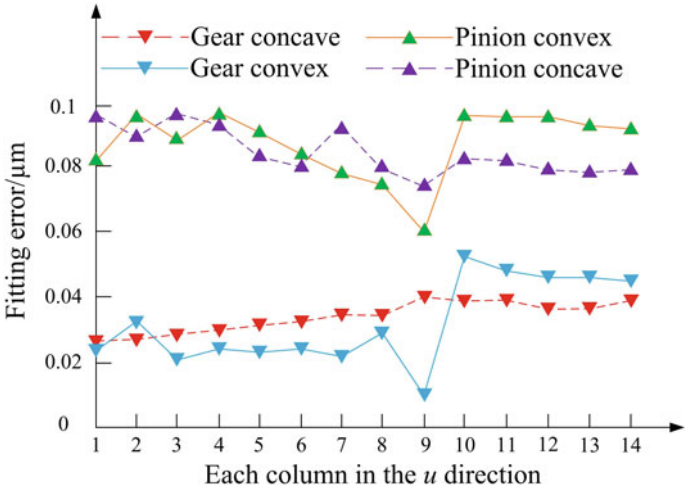

Fig. 1.4 Fitting error curve

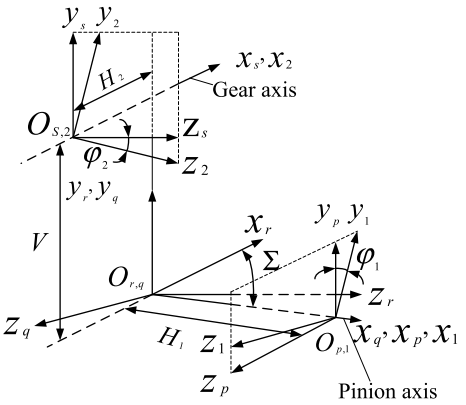

Fig. 1.5 Meshing coordinate systems

$$= M_{s1} P_1(u_1, v_1) \tag{1.3}$$

$$M_{s\_p2} = M_{s2} P_2(u_2, v_2) \tag{1.4}$$

where

$$M_{p1} = \begin{bmatrix} 1 & 0 & 0 & 0 \\ 0 & \cos(\varphi_1) & \sin(\varphi_1) & 0 \\ 0 & -\sin(\varphi_1) & \cos(\varphi_1) & 0 \\ 0 & 0 & 0 & 1 \end{bmatrix}$$

$$M_{qp} = \begin{bmatrix} 1 & 0 & 0 & H_1 \\ 0 & 1 & 0 & 0 \\ 0 & 0 & 1 & 0 \\ 0 & 0 & 0 & 1 \end{bmatrix}$$

$$M_{rq} = \begin{bmatrix} \cos(\Sigma) & 0 & -\sin(\Sigma) & 0 \\ 0 & 1 & 0 & 0 \\ \sin(\Sigma) & 0 & \cos(\Sigma) & 0 \\ 0 & 0 & 0 & 1 \end{bmatrix}$$

$$M_{sr} = \begin{bmatrix} 1 & 0 & 0 & H_2 \\ 0 & 1 & 0 & -V \\ 0 & 0 & 1 & 0 \\ 0 & 0 & 0 & 1 \end{bmatrix}$$

$$M_{s2} = \begin{bmatrix} 1 & 0 & 0 & 0 \\ 0 & \cos(\varphi_2) & \sin(\varphi_2) & 0 \\ 0 & -\sin(\varphi_2) & \cos(\varphi_2) & 0 \\ 0 & 0 & 0 & 1 \end{bmatrix}$$

φ_1 and φ_2 are the rotary angles of pinion and gear. M_{s1} and M_{s2} are the transformation matrices from measuring coordinate system S_1 and S_2 to the meshing coordinate system S_s for the pinion and gear. S_p, S_q, and S_r are auxiliary coordinate systems. H_1 and H_2 are the axial settings of pinion and gear. Σ is the shaft angle. V is the pinion offset distance.

1.4.2 Meshing Point Calculation and Contact Pattern Search

During the rolling test, the tooth surface needs to be coated with some red lead powder that diameter is 0.00635 mm [10]. when the red lead powder is in the area where the gap is less than 0.00635 mm, the red lead powder will be crushed, and this area becomes the contact pattern. Therefore, this study refers to this idea and proposes a new digital rolling test method based on the real tooth surface. This method consists of two parts: meshing point calculation and contact pattern search.

The content of the contact pattern search is as follows: the gear is discretized into grids. When two tooth surfaces are in a meshing state, the shortest distance from each grid point of the gear to the tooth surface of the pinion is calculated, and all grid points with the shortest distance less than 0.00635 mm are searched out. The outline of the grid point is considered to be in contact ellipse.

The calculation process of the meshing point is as follows:

Step 1: Discrete grid of tooth surface. The tooth surface of the gear is discretized into a dense grid, and then the three-dimensional coordinates of the grid points are obtained. The pinion tooth grid uses a 15 × 15 measuring grid.
Step 2: Position adjustment of the tooth surfaces of the gear. By rotating φ_2 in a clockwise direction, there is at least one grid point on the gear and the normal vector passing this point intersects the pinion tooth surface, as shown in Fig. 1.6a.
Step 3: Judgment of the grid where the intersection point is located. The intersection point may fall on any of the 14 × 14 pinion tooth surface patches, so it is necessary to determine the grid where the intersection point is located. The judgment is based on the following: there will be four angles when the intersection point is connected to the four corner points of the surface patch. If the four angles add up to 360°, it can be considered that the point is in the grid patch, as shown in Fig. 1.6b. If the sum of the four angles does not equal 360°, it falls outside the surface patch. Starting from the first surface patch, until this surface patch is found by the above method. When the surface patch is determined, the equation of the NURBS surface can accurately express the equation of the surface patch. According to the formula of the shortest distance from the point to the surface, the shortest distance d_{min} is calculated from the grid points on the gear to the tooth surface of the pinion.
Step 4: Calculation of the meshing point. When the shortest distance d_{min} is calculated from each grid point on the gear to the tooth surface of the pinion, find out the minimum value D_{min} from the shortest distance d_{min}. (As shown in Fig. 6c, $d'_{\min}$ and $d''_{\min}$ are the d_{min} at different positions). The minimum value D_{min} will correspond to three different meshing situations.

i. If this minimum value D_{min} is less than 0.01 μm and other positions do not interfere, this point is considered to be the meshing point. Search for gear grid points with the shortest distance d_{min} less than 0.00635 mm around the meshing point, and then the outline of the searched area is the contact ellipse. Then perform step 6.
ii. If the minimum value D_{min} is less than 0.01 μm but there is interference, it means that the rotation angle φ_2 is too large, and it is necessary to reduce the rotation angle φ_2, and the detailed process performs step 5.
iii. If the minimum value D_{min} is not less than 0.01 μm, the reason is that the grid is too sparse or the rotation angle φ_2 is too small. The method of solution is to perform local grid refinement near the minimum value $D_{\min}$ on the gear, and then the shortest distance $d_{\min}$ corresponding to all the refined grid points and the minimum value $D_{\min}$ are calculated again, as shown in Fig. 1.6d. Observe the change of the minimum value $D_{\min}$, if the decreased amplitude value of $D_{\min}$ is more than 1%, the grid continues to be refined; if the decreased amplitude value of $D_{\min}$ is less than 1%, and then program adjusts rotation angle φ_2 according to formula (1.5) in the clockwise direction. Finally, the program performs step 3.

$$h = k \cdot D_{\min} \tag{1.5}$$

where k is the step length coefficient, h is the adjustment step length.

Step 5: Adjustment of the rotation angle φ_2. The rotation angle φ_2 needs to be adjusted in a counterclockwise direction by the formula (1.5) since the rotation angle φ_2 is too large, and then the program performs step 3. The flow chart is shown in Fig. 1.7.

Step 6: Calculation of the meshing point at the next moment. When the two meshing surfaces are engaged at the next moment, the rotation angles φ_1 and φ_2 may not exactly match the theoretical transmission ratio due to errors in the model. So it is still necessary to calculate the meshing point from step 3.

Step 7: Calculation of transmission error. The real rotation angles and theoretical rotation angles will be calculated for each meshing point position according to the above method for the pinion and gear. Then the transmission error can also be calculated by the following formula:

$$\Delta E = (\varphi_2 - \varphi_{20}) - \frac{Z_1}{Z_2}(\varphi_1 - \varphi_{10}) \tag{1.6}$$

where φ_{10} and φ_{20} are the initial rotation angles of pinion and gear respectively. φ_1 and φ_2 are the real rotation angles of pinion and gear respectively. Z_1 and Z_2 are the teeth numbers of pinion and gear respectively.

1.5 Calculation Examples and Comparative Analysis

The tooth surface meshing and contact simulation program was compiled based on the above method. Still taking the gear model that has been built above as an example. With using of the digital rolling test in this study, the contact pattern and the transmission error curve of the gear are obtained, as shown in Fig. 1.8.

By comparing Figs. 1.8 and 1.9, the contact pattern obtained by the method is similar to the simulation results of the Ref. [11] in terms of size, shape, and position. There are some differences in shape by comparing each instant contact ellipse, the reason is caused by the pattern search. According to the description in Ref. [12], the contact ellipse obtained by searching is different from the standard contact ellipse. Because the search method avoids the quadratic approximation and curvature derivation of the tooth surface, the instant contact ellipse obtained by the search method can better reflect the actual contact situation of the tooth surface. So these differences are allowed. Compare the contact pattern in Fig. 1.8 with the contact pattern in Fig. 1.9, the actual pattern boundary at the tooth root of this study is higher than the pattern boundary of the Ref. [11]. And the reason is that the meshing area is bounded by the transition curve of the tooth root of the gear tooth surface instead of the tip of the pinion.

By comparing Fig. 1.6c in Figs. 1.8 and 1.9, the shape of the transmission error curve is similar, and the relative error value is 6.67%, as shown in Table 1.4. By

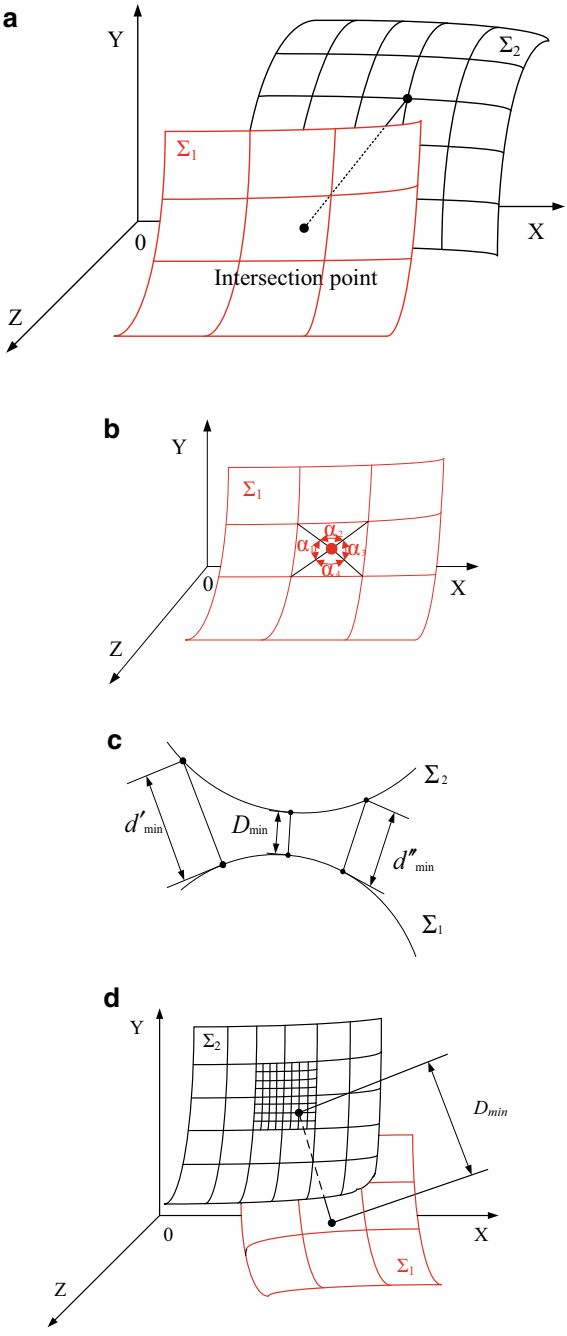

Fig. 1.6 Schematic diagram of the calculation process of the meshing point. **a** Schematic diagram of intersection of gear grid point normal vector and pinion tooth surface. **b** Schematic diagram of intersection location judgment. **c** Schematic diagram of the shortest distance. **d** Schematic diagram of partial encryption

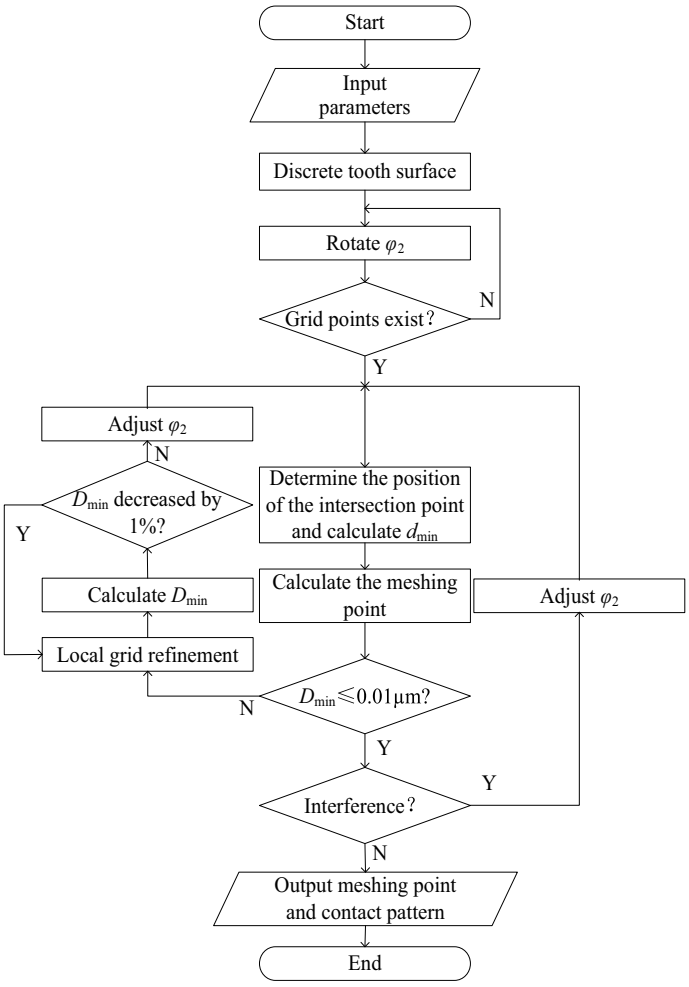

Fig. 1.7 Flow chart of the digital rolling test method

comparing Fig. 1.6d in Figs. 1.8 and 1.9, there is a difference in the shape of the transmission error curve, and the relative error value is 10.1%. The reason for this error is the tooth surface modeling error.

It should be noted that this study takes the point on the theoretical tooth surface of the Ref. [11] as an example and compares results with the simulation results of the Ref. [11]. This does not affect the application of the method to the fitting of the measuring data and meshing simulation analysis for the real tooth surface.

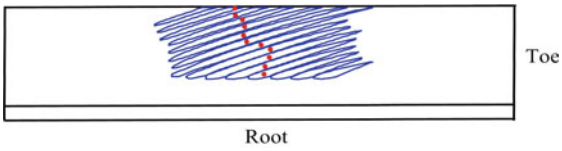

(a) Contact pattern of the gear convex

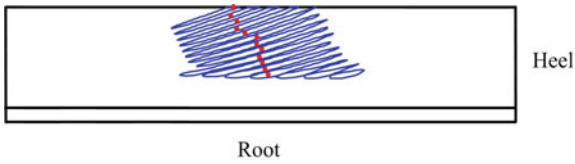

(b) Contact pattern of the gear concave

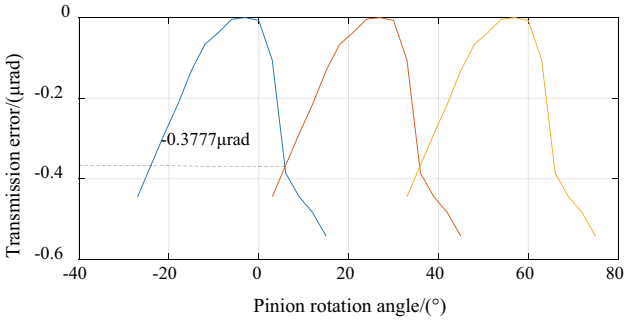

(c) Transmission error of the drive side

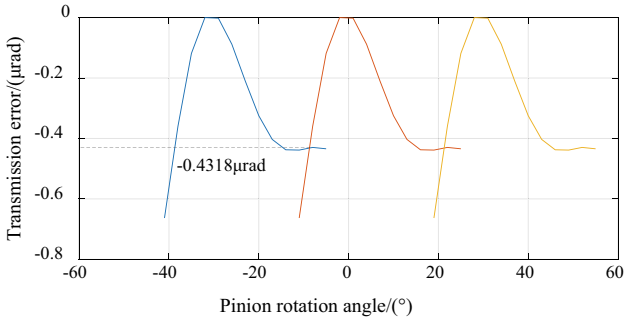

(d) Transmission error of the coast side

Fig. 1.8 Result of the digital rolling test method

Fig. 1.9 Theoretical results of the tooth contact analysis

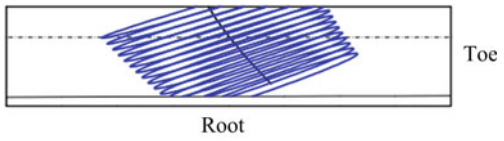

(a) Theoretical contact pattern of the gear convex

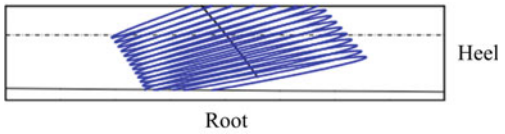

(b) Theoretical contact pattern of the gear concave

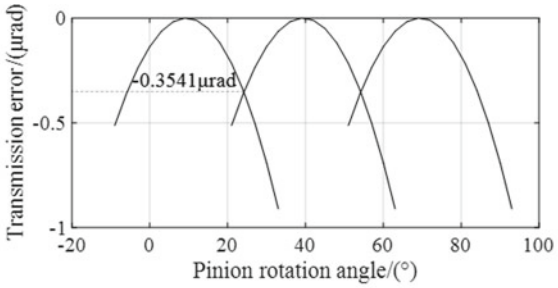

(c) Theoretical transmission error of the drive side

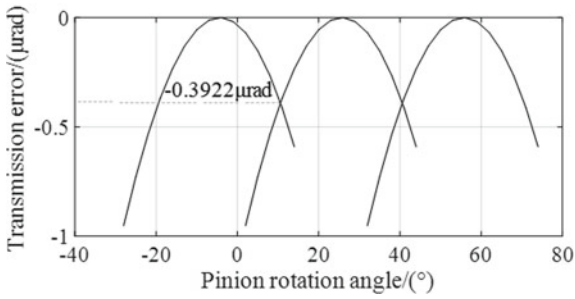

(d) Theoretical transmission error of the coast side

Table 1.4 Transmission error comparison

Items	Drive side	Coast side
Digital rolling test method/(μrad)	−0.3777	−0.4318
Theoretical method/(μrad)	−0.3541	−0.3922
Relative error (%)	6.67	10.1

1.6 Conclusions

(1) This study proposes a gear digital rolling test method based on the actual measured tooth surface. Compared with the traditional method of tooth contact analysis, the method of this study does not rely on the derivation of the complicated principal curvature and principal direction and does not rely on the quadratic approximation of the curved surface. Therefore, the result obtained is closer to the actual meshing situation.
(2) This method use the measuring point and is applied to the real tooth surface with machining errors and heat treatment deformation. It provides an effective way to analyze the meshing law of the real tooth surface without the rolling test, which is beneficial to the closed-loop manufacturing of gears.

Acknowledgments This project is supported by National Natural Science Foundation of China (Grant No. 51705419), China Postdoctoral Science Foundation (Grant No. 2018M633540), and Natural Science Basic Research Plan in Shaanxi Province of China (Grant No. 2017JQ5048).

References

1. Zhuo, Y.B., Zhou, X.J., Lu, H.L., et al.: Theoretical and experimental investigation on contact characteristics of hypoid gears under quasi-static condition. Chin. J. Sci. Instrum. **38**(05), 1285–1295 (2017). (in Chinese)
2. Wang, X., Fang, Z.Z., Mu, Y.M., et al.: Optimization design of loaded transmission error for HGT hypoid gear drives. J. Vibr. Shock **36**(08), 34–40 (2017). (in Chinese)
3. Litvin, F.L.: Applied theory of gearing: state of the art. J. Vibr. Acoustics Trans. ASME **117**(B), 128 (1995)
4. Sun, D.Z.: The Real Tooth Surface Meshing Theory, pp. 62–87. Science Press, Beijing (2006) (in Chinese)
5. Su, Z.J., Wu, X.T., Mao, S.M., et al.: Design of hypoid gear tooth surface represented by non-uniform rational b-spline polynomial. J. Xi'an Jiaotong Univ. **039**(1), 17–20 (2009). (in Chinese)
6. Liu, G.L., Chang, K.: The high precision numerical simulation of spiral bevel gear tooth surface meshing analysis. Aero Engine **39**(02), 19–24 (2013). (in Chinese)
7. Zhang, J.H., Fang, Z.D., Wang, C.: Digital simulation of spiral bevel gears' real tooth surfaces based on non-uniform rational B-spline. J. Aerospace Power **24**(7), 1672–1676 (2009). (in Chinese)
8. Du, J.F., Fang, Z.D., Gao, H.B., et al.: Analysis of real tooth surface contact of cycloidal hypoid gear. J. South China Univ. Technol. **43**(3), 35–40 (2015). (in Chinese)
9. Wang, Z.R., Du, J.F., Liu, K., et al.: An Improved gear geometry contact simulation method. J. Mech. Trans. **42**(11), 76–79 (2018). (in Chinese)
10. Fan, Q.: Enhanced algorithms of contact simulation for hypoid gear drives produced by face-milling and face-hobbing peocesses. J. Mech. Des. **129**, 31–37 (2007)
11. Shi, Y.B.: Study on the Flank Modification of Face Hobbed Hypoid Gears, p. 48. National Chung Cheng University, Taiwan (2004) (in Chinese)
12. Du, J.F., Wang, Z.R., Liu, K., et al.: A novel tooth contact analysis method based on value iteration. Mech. Mach. Sci. **77**, 162–169 (2020)

Yongxiang Liu born in 1994, is currently a master candidate at the School of Mechanical and Precision Instrument Engineering, Xi'an University of Technology, China.

Jinfu Du born in 1984, is currently an associate professor at Xi'an University of TechnologyChina. He received his Ph.D. degree from Northwestern Polytechnical University, China, in 2015. His research interests include advanced design and manufacturing techniques of gear transmission.

Kai Liu born in 1958, is currently a professor and Ph.D. candidate supervisor at the School of Mechanical and Precision Instrument Engineering, Xi'an University of Technology, China. His main research interests include the theory and application of mechanical drive and vehicle engineering.